Neurosci. Bull. December, 2020, 36(12):1441–1453
https://doi.org/10.1007/s12264-020-00568-6

www.neurosci.cn
www.springer.com/12264

ORIGINAL ARTICLE

Spinal Cord Stimulation Enhances Microglial Activation in the Spinal Cord of Nerve-Injured Rats

Bin Shu[1,2] · Shao-Qiu He[1] · Yun Guan[1,3]

Received: 30 April 2020 / Accepted: 23 July 2020 / Published online: 5 September 2020

Abstract Microglia can modulate spinal nociceptive transmission. Yet, their role in spinal cord stimulation (SCS)-induced pain inhibition is unclear. Here, we examined how SCS affects microglial activation in the lumbar cord of rats with chronic constriction injury (CCI) of the sciatic nerve. Male rats received conventional SCS (50 Hz, 80% motor threshold, 180 min, 2 sessions/day) or sham stimulation on days 18–20 post-CCI. SCS transiently attenuated the mechanical hypersensitivity in the ipsilateral hind paw and increased OX-42 immunoreactivity in the bilateral dorsal horns. SCS also upregulated the mRNAs of M1-like markers, but not M2-like markers. Inducible NOS protein expression was increased, but brain-derived neurotrophic factor was decreased after SCS. Intrathecal minocycline (1 μg–100 μg), which inhibits microglial activation, dose-dependently attenuated the mechanical hypersensitivity. Pretreatment with low-dose minocycline (1 μg, 30 min) prolonged the SCS-induced pain inhibition. These findings suggest that conventional SCS may paradoxically increase spinal M1-like microglial activity and thereby compromise its own ability to inhibit pain.

✉ Yun Guan
yguan1@jhmi.edu

[1] Department of Anesthesiology and Critical Care Medicine, School of Medicine, Johns Hopkins University, Baltimore, MD 21205, USA

[2] Present Address: Department of Anesthesiology, Tongji Hospital, Tongji Medical College, Huazhong University of Science and Technology, Wuhan 430030, China

[3] Department of Neurological Surgery, School of Medicine, Johns Hopkins University, Baltimore, MD 21205, USA

Keywords Spinal cord stimulation · Microglia · Neuropathic pain · Spinal cord · Rat

Introduction

Glial cells, including both macroglia and microglia, account for ~70% of the cells in the central nervous system (CNS) [1]. These cells play important roles in maintaining homeostasis, supporting and protecting neurons, and synthesizing and releasing various neuromodulators that affect neuronal excitability. Microglia, the resident innate immune cells of the CNS, show remarkable morphological and functional plasticity to environmental changes, injuries, and neurologic disorders [2–4]. Both quiescent and activated microglia have been isolated from the CNS by immunomagnetic separation [3]. The isolated microglia retain properties similar to those *in vivo*, and hence are suitable for use in *ex vivo* investigations [2, 3]. The phenotypes of isolated microglia also correlate with two major phenotypic profiles characterized mostly by *in vitro* studies. The classically activated M1-like state is associated with the release of pro-inflammatory cytokines [e.g., tumor necrosis factor (TNF)-α, interleukin (IL)-1β, and IL-6], which are thought to enhance pain transmission and exacerbate neurological injury [4–6]. The alternative anti-inflammatory M2-like state mediates neuronal repair, neurogenesis, and protection against neurotoxicity and is associated with the release of anti-inflammatory cytokines (e.g., IL-10 and IL-4) [4]. Mounting evidence suggests that activation of microglia and astrocytes in the spinal cord contributes to pain facilitation and exacerbation, such as that experienced after tissue and nerve injury [4, 5, 7, 8].

An important strategy for treating pain when pharmacotherapies fail or cause intolerable side-effects is spinal cord stimulation (SCS) [9]. Conventional SCS, which has

been used for over 50 years, activates low-threshold Aβ-fibers in the dorsal columns and induces pain inhibition through both spinal and supraspinal neuronal mechanisms [10–13]. Although it is useful, conventional SCS is associated with suboptimal clinical efficacy and short-lived pain relief [14]. Until recently, attempts to improve SCS have focused primarily on neuronal effects [11, 13–17]. Intriguingly, a new SCS paradigm with differential target multiplexed programming (DTMP) produced better pain inhibition than conventional SCS, and more effectively modulated glia-related genes and pain-relevant biological processes associated with neuron-glial interactions in nerve-injured rats [18]. Despite the ability of glial cells to initiate signaling cascades that modulate neuronal excitability and pain processing, glial mechanisms have often been overlooked in the study of SCS.

A previous study showed that conventional SCS decreases glial cell reactivity markers in the spinal cord of nerve-injured rats, indicating glial suppression [19]. Yet, recent genome-wide microarray and RNA-sequencing studies have suggested that SCS may increase immune responses and promote glial activation in the spinal cord of neuropathic rats [20–22]. Microarray and RNA-sequencing studies are useful for identifying gene networks that are altered by SCS, but they reveal changes in gene expression only at the transcriptional level. Accordingly, the effects of conventional SCS on activation of spinal glial cells in neuropathic pain are still unknown. By conducting animal behavioral tests, immunocytochemistry, real-time polymerase chain reaction (RT-PCR), and western blot analysis, we endeavored to determine how conventional SCS affects microglial activation and alters the expression of pro-inflammatory (M1-like) and anti-inflammatory (M2-like) phenotypic markers in the lumbar spinal cord after sciatic nerve injury in male rats.

Materials and Methods

All procedures were approved by the Johns Hopkins University Animal Care and Use Committee (Baltimore, MD, USA) as consistent with the National Institutes of Health Guide for the Care and Use of Laboratory Animals to ensure minimal animal use and discomfort. Animals received food and water *ad libitum* and were maintained on a 12-h day–night cycle in isolator cages.

Animals and Surgery

Animals

Adult, male Sprague-Dawley rats (2–3 months old, Harlan Bioproducts for Science, Indianapolis, IN) were administered SCS and drug treatment for behavioral tests and molecular biological studies.

Chronic Constriction Injury (CCI) of Sciatic Nerve

A neuropathic pain model of CCI was made as described previously [23]. Briefly, animals were anesthetized with 2.0% isoflurane (Abbott Laboratories, North Chicago, IL). The left sciatic nerve was loosely ligated with a 6–0 silk suture. The animals were monitored after surgery for signs of wound infection, inadequate food and water intake, or weight loss until the surgical site had healed.

Behavioral Tests

Mechanical Hypersensitivity Test

Hypersensitivity to punctuate mechanical stimulation was determined with the up-down method by using a series of von Frey filaments (0.38 g, 0.57 g, 1.23 g, 1.83 g, 3.66 g, 5.93 g, 9.13 g, and 13.1 g) [24]. Briefly, the von Frey filaments were applied to the test area between the footpads on the plantar surface of the hind paw for 4 s to 6 s. If a positive response occurred (abrupt paw withdrawal, licking, and shaking), the next smaller von Frey hair was used; if a negative response was observed, the next higher force was used. The test was continued until (1) the responses to five stimuli were assessed after the first crossing of the withdrawal threshold or (2) the upper/lower end of the von Frey hair set was reached before a positive/negative response had been obtained. The paw withdrawal threshold (PWT) was determined according to the formula provided by Dixon [25]. Rats that showed impaired motor function after surgery or that failed to develop mechanical hypersensitivity (mechanical allodynia, >50% reduction from pre-CCI PWT) on the hind paw ipsilateral (left) to the nerve injury by day 5 post-injury were excluded from subsequent study.

SCS in CCI Rats

One week after CCI, a custom-made quadripolar electrode (contact diameter, 0.9 mm–1.0 mm; center spacing, 2.0 mm; Medtronic Inc., Minneapolis, MN) that provided bipolar SCS ("twin-pairs" stimulation) was placed epidurally through a small laminectomy at the T13 vertebra (Fig. 1A), as described in our previous studies [16, 21]. The sterilized lead was placed at the T10–12 levels, which correspond to the T13–L1 spinal cord region. A subcutaneous tunnel was used to position the proximal end of the electrode in the upper thoracic region, where it exited the skin and connected to an external stimulator (Model 2100, A-M Systems, Sequim, WA). Animals were allowed to

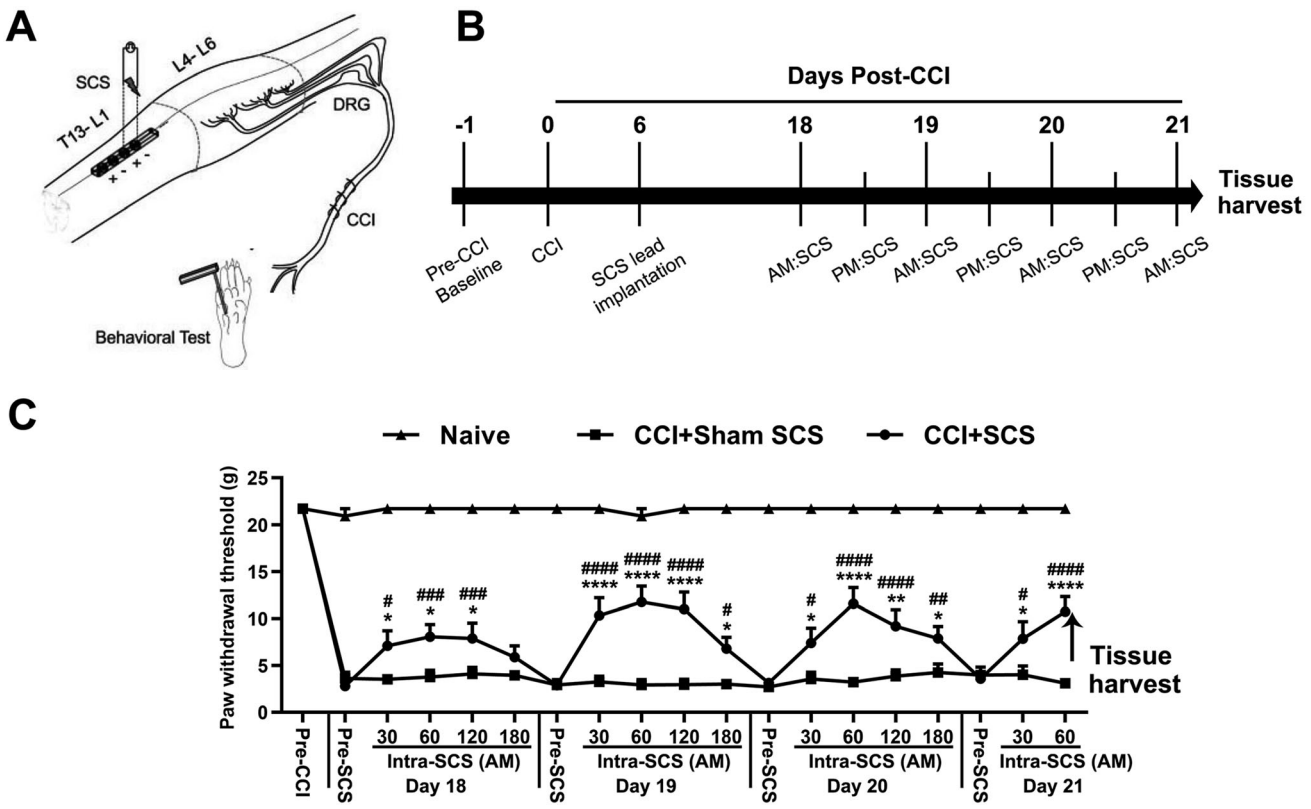

Fig. 1 Repeated SCS induces short-term inhibition of mechanical hypersensitivity in CCI rats. **A** Schematic illustrating the experimental setup for repeated SCS in rats with CCI of the left sciatic nerve. Lumbar spinal cord tissue (L4–L6, marked with dotted lines) ipsilateral to the side of nerve injury was harvested after the last SCS treatment on day 21 post-injury. **B** Experimental timeline. CCI rats received repeated SCS (50 Hz, 0.2 ms, biphasic, 80% motor threshold, 180 min/session, $n = 15$) or sham stimulation ($n = 10$) from days 18 to 21 post-injury. Naïve rats ($n = 8$) received no treatment. **C** Paw withdrawal thresholds were measured before injury (Pre-CCI), before stimulation (Pre-SCS), and during the morning (AM) session of SCS (Intra-SCS) on days 18 to 21 post-injury. Data are shown as the mean ± SEM. Two-way mixed model ANOVA, with Bonferroni *post hoc* test. $^{*}P < 0.05$, $^{**}P < 0.01$, $^{****}P < 0.0001$ *versus* CCI+Sham SCS; $^{\#}P < 0.05$, $^{\#\#}P < 0.01$, $^{\#\#\#}P < 0.001$, $^{\#\#\#\#}P < 0.0001$ *vs* Pre-SCS of the same day.

recover from surgery for >1 week. SCS and mechanical pain hypersensitivity were examined at 7 days–14 days after lead implantation (Fig. 1B).

CCI rats were randomized to receive SCS ($n = 15$) or sham stimulation ($n = 10$). On each test day, rats were acclimated for 30 min before we measured the pre-SCS PWT. Motor threshold (MoT), which ranged from 0.1 mA to 0.5 mA, was determined first by slowly increasing the amplitude of 4 Hz electrical stimulation from zero until muscle contraction was observed in mid-lower trunk or hind limbs. On days 18, 19, and 20 post-CCI, rats received SCS (50 Hz, 0.2 ms, biphasic, constant current, 80% MoT, 180 min) or sham stimulation (0 mA) in two sessions per day, and on day 21, they received one session in the morning. We measured PWT before applying SCS and at 30 min, 60 min, 120 min, and 180 min during SCS (intra-SCS) on days 18 to 20 in the morning session, and at 30 min and 60 min during SCS on day 21 (Fig. 1B). We used 80% MoT because it represents the maximum intensity of SCS that can be applied without causing discomfort in awake animals and has been used in previous studies [16, 20, 26]. Naïve rats ($n = 8$) received neither CCI nor SCS treatment and were handled and tested in parallel with other groups of rats.

Immunocytochemistry

Rats were deeply anesthetized with isoflurane (2%–3%) at 1–2 h after the last SCS treatment and perfused intracardially with 0.1 mol/L phosphate-buffered saline (PBS; pH 7.4, 4°C) followed by fixative (4% formaldehyde and 14% [*v*/*v*] saturated picric acid in PBS, 4°C). Lumbar (L4–L6) spinal cord tissue was cryoprotected in 20% sucrose for 24 h before being serially cut into 15-µm sections and placed on slides. The slides were incubated overnight at 4°C in the primary antibodies mouse antibody to glial fibrillary acidic protein (GFAP; MAB-360, 1:500, Millipore, Temecula, CA) and mouse OX-42 antibody (CBL-1512, 1:500, Millipore). Slides were incubated in secondary antibody at room temperature for 45 min. The secondary antibody,

donkey antibody to mouse (715-095-151, FITC-conjugated, Jackson ImmunoResearch, West Grove, PA), was diluted 1:100 in PBS. Tissues from different experimental groups were processed and analyzed simultaneously. The images of immunostained tissue were analyzed with ImageJ 1.46a (NIH, Bethesda, MD). Areas that contained positive immunoreactivity are expressed as percentage of total dorsal horn on each side.

Real-Time PCR

The dorsal aspect of the lumbar (L4–L6) spinal cord was collected from naïve and CCI rats at 1 h–2 h after the last SCS. Tissues ipsilateral and contralateral to the nerve injury were then separated. Half of the tissue on each side was used for RT-PCR, and the other half was processed for western blot analysis. RNA and protein were isolated using TRIzol reagent (Invitrogen, Carlsbad, CA) according to the manufacturer's protocols. After measuring the concentration of RNA on a Nanodrop 2000c (Thermo Fisher, Waltham, MA), we prepared cDNA from 1 μg of total RNA using an oligo(dT) primer and reverse transcriptase (SuperScript III First-Strand Synthesis SuperMix for qRT-PCR, 11752-050, Invitrogen, CA) according to the kit instructions. PowerUp SYBR Green Master Mix (A25741, Applied Biosystems, Waltham, MA) was used to perform real-time PCR on the StepOnePlus Real-Time PCR system (Applied Biosystems). Each PCR mixture contained 500 nmol/L forward and reverse primers, 5 μL of PowerUp SYBR Green Master Mix (2X), 1 μL of cDNA, and 2 μL of nuclease-free water for a total volume of 10 μL. PCR was carried out with the following steps: uracil-DNA glycosylase activation at 50°C for 2 min, Dual-Lock DNA polymerase at 95°C for 2 min, denature at 95°C for 15 s, anneal at 55°C–60°C for 15 s, and extend at 72°C for 1 min. All PCRs were performed in triplicate; β-actin was used as an endogenous control and to normalize the mRNA expression data. Relative expression was calculated by the $2^{-\Delta\Delta Ct}$ method. Primer sequences are listed in Table 1.

Western Blot Analysis

Protein was isolated using a TRIzol reagent kit and concentration determined by the bicinchoninic acid method (Thermo Fisher). After protein concentrations were equalized with 1% sodium dodecyl sulfate (SDS), 4X Bolt lithium dodecyl sulfate sample buffer (Thermo Fisher) and 10X Bolt sample reducing agent (Thermo Fisher) were added to the samples in a ratio of 1 to 1. Finally, the samples were heated at 70°C for 10 min and separated by electrophoresis on 4%–12% Bis-Tris Plus SDS-polyacrylamide gels at a constant voltage for ~35 min in Bolt 2-(N-morpholino) ethanesulfonic acid SDS running buffer. Protein was transferred to a polyvinylidene difluoride membrane (Bio-Rad, Berkeley, CA) and blocked in a solution of tris-buffered saline and 0.1% Tween 20 containing 5% nonfat dry milk (Bio-Rad). Membranes were incubated with mouse anti-inducible nitric oxide synthase (iNOS) antibody (1:1000, BD Biosciences, San Jose, CA), rabbit anti-TNF-α antibody (1:1000, Abcam, Cambridge, UK), goat anti-arginase 1 (Arg1) antibody (1:1000, Santa Cruz Biotechnology, Dallas, TX), rabbit anti-IL10 antibody (1:1000, Abcam), rabbit anti-phosphorylated extracellular signal-regulated kinase (p-ERK1/2) antibody (1:2000, Cell Signaling Technology, Danvers, MA), rabbit anti-c-Fos antibody (1:1000, Abcam), rabbit anti-protein kinase C (PKC)-γ antibody (1:1000, Santa Cruz Biotechnology), rabbit anti-brain derived neurotrophic factor (BDNF) antibody (1:800, Santa Cruz Biotechnology), rabbit anti-phosphorylated glutamate receptor (p-GluR) subunit 1 at serine 831 residue (p-GluR1^{ser831}) antibody (1:1000, Millipore), rabbit anti-phosphorylated N-methyl-D-aspartate (NMDA) receptor 1 (p-NR1) antibody (1:1000, Millipore), or rabbit anti-glyceraldehyde 3-phosphate dehydrogenase antibody (1:100,000, Millipore). Peroxidase-conjugated goat anti-mouse IgG, goat anti-rabbit IgG, and donkey anti-goat IgG (1:10,000, Jackson ImmunoResearch, West Grove, PA) were used as secondary antibodies. Membranes were incubated in enhanced chemiluminescence (Bio-Rad) and imaged by ImageQuant LAS 4000 (GE Healthcare Life Sciences). Protein band densities were analyzed with ImageJ 1.46a software.

Drugs and Intrathecal Injections

Minocycline from Tocris Bioscience (Bristol, UK) was dissolved in water to 25 mmol/L, separated into aliquots, and stored in tightly-sealed vials at −20°C. This stock solution was freshly diluted to the desired dosage with vehicle (saline) before use. Rats were briefly anesthetized in 2.0% isoflurane before being infused intrathecally with drug or vehicle *via* lumbar puncture [27]. CCI rats were randomized to receive a 15 μL intrathecal injection of vehicle ($n = 7$) or minocycline (1 μg, $n = 9$; 10 μg, $n = 10$; or 100 μg, $n = 9$) at day 18 post-CCI. PWT was tested 1 day before CCI, before intrathecal injection (pre-IT), and 30 min, 60 min, 120 min, 150 min, 180 min, and 240 min after injection (post-IT).

Data Analysis

To determine the PWT in animal behavior studies, we converted the pattern of positive and negative von Frey filament responses to a 50% threshold value using the formula provided by Dixon [25]. The PWT was compared

Table 1 Primers used for RT-PCR.

Gene	Forward primer (5′-3′)	Reverse primer (5′-3′)
Astrocyte marker		
GFAP	TCCTGGAACAGCAAAACAAG	CAGCCTCAGGTTGGTTCAT
Microglial marker		
OX42	CAGATCAACAATGTGACCGTATGGG	CATCATGTCCTTGTACTGCCGCTTG
M1 markers		
iNOS	CCCTTCAATGGTTGGTACATGG	ACATTGATCTCCGTGACAGCC
CD16	GCTTTCTACCGTGGCATCA	TCCAGTGAAGTTTGGGTTCC
CD32	TGAAGAAGGGGAAACCATCA	GGCTTTGGGGATTGAAAAAT
M2 markers		
Arg1	TTAGGCCAAGGTGCTTGCTGCC	TACCATGGCCCTGAGGAGGTTC
CD163	TGGGCAAGAACAGAATGGTT	CCTGAGTGACAGCAGAGACG
TGF-β	GACCTGCTGGCAATAGCTTC	GACTGGCGAGCCTTAGTTTG
Pro-inflammatory cytokines		
TNF-α	TGAGCACTGAAAGCATGATCC	GGAGAAGAGGCTGAGGAACA
IL-1β	CAGGAAGGCAGTGTCACTCA	AAAGAAGGTGCTTGGGTCCT
Anti-inflammatory cytokines		
IL-4	CAGGGTGCTTCGCAAATTTTAC	CACCGAGAACCCCAGACTTG
IL-10	TAAGGGTTACTTGGGTTGC	TATCCAGAGGGTCTTCAGC
Control		
β-Actin	AGAAGGACTCCTATGTGGGTGA	CATGAGCTGGGTCATCTTTTCA

between the pre- and post-SCS conditions and between groups by using a two-way mixed model analysis of variance (ANOVA). In each study, we blinded the experimenter to the treatments (e.g., drug) to reduce selection and observation bias. Western blot and immunocytochemistry data were analyzed as described previously [28, 29]. The ipsilateral and contralateral spinal cord were analyzed separately, and results from different groups were compared. Statistica 6.0 software (StatSoft, Inc., Tulsa, OK) was used to conduct all statistical analyses. The Tukey honestly significant difference *post hoc* test was used to compare specific data points. Bonferroni correction was applied for multiple comparisons. Two-tailed tests were performed and numerical data expressed as the mean + SEM; $P < 0.05$ was considered statistically significant in all tests.

Results

SCS Induces Inhibition of Mechanical Hypersensitivity in CCI Rats

The PWT of the ipsilateral hind paw was significantly decreased from the pre-injury level in CCI rats before SCS treatment on day 18 post-CCI (Fig. 1C; $F = 201.1$, group; $F = 18.84$, time; $F = 6.66$, group–time interaction). SCS ($n = 15$) increased the ipsilateral PWTs of CCI rats from the pre-SCS level on each of the treatment days. The pain-inhibiting effect started by 30 min intra-SCS and peaked ~60 min intra-SCS. Sham SCS ($n = 10$) did not significantly alter the PWT in CCI rats.

SCS Enhances Microglial Activation in the Spinal Cord of CCI Rats

Sham-stimulated CCI rats exhibited significantly greater immunoreactivity for both GFAP (an astrocyte-reactive marker) and OX-42 (a microglia-reactive marker) than did naïve rats (Fig. 2A, B). Repeated SCS treatment induced a downward trend in the GFAP immunoreactivity of CCI rats that was not seen in sham-stimulated rats ($P = 0.38$). GFAP immunoreactivity on the contralateral side was not significantly altered by CCI or SCS (Fig. 2A). In contrast, SCS produced a significant increase in OX-42 immunoreactivity in both the ipsilateral and contralateral dorsal horn of CCI rats, when compared to that in sham-stimulated rats (Fig. 2B). RT-PCR revealed that the levels of GFAP and OX-42 mRNA in the ipsilateral lumbar cord were approximately two-fold higher in sham-stimulated CCI rats than in naïve rats (Fig. 2C, D). CCI rats that received SCS showed a trend toward an additional increases in OX-42 mRNA ($P = 0.06$) but no change in GFAP mRNA (Fig. 2A: $F = 22.29$, ipsilateral; $F = 4.203$, control; Fig. 2B, $F = 23.10$, ipsilateral; $F = 6.64$, control; Fig. 2C: $F = 4.37$; Fig. 2D; $F = 9.52$).

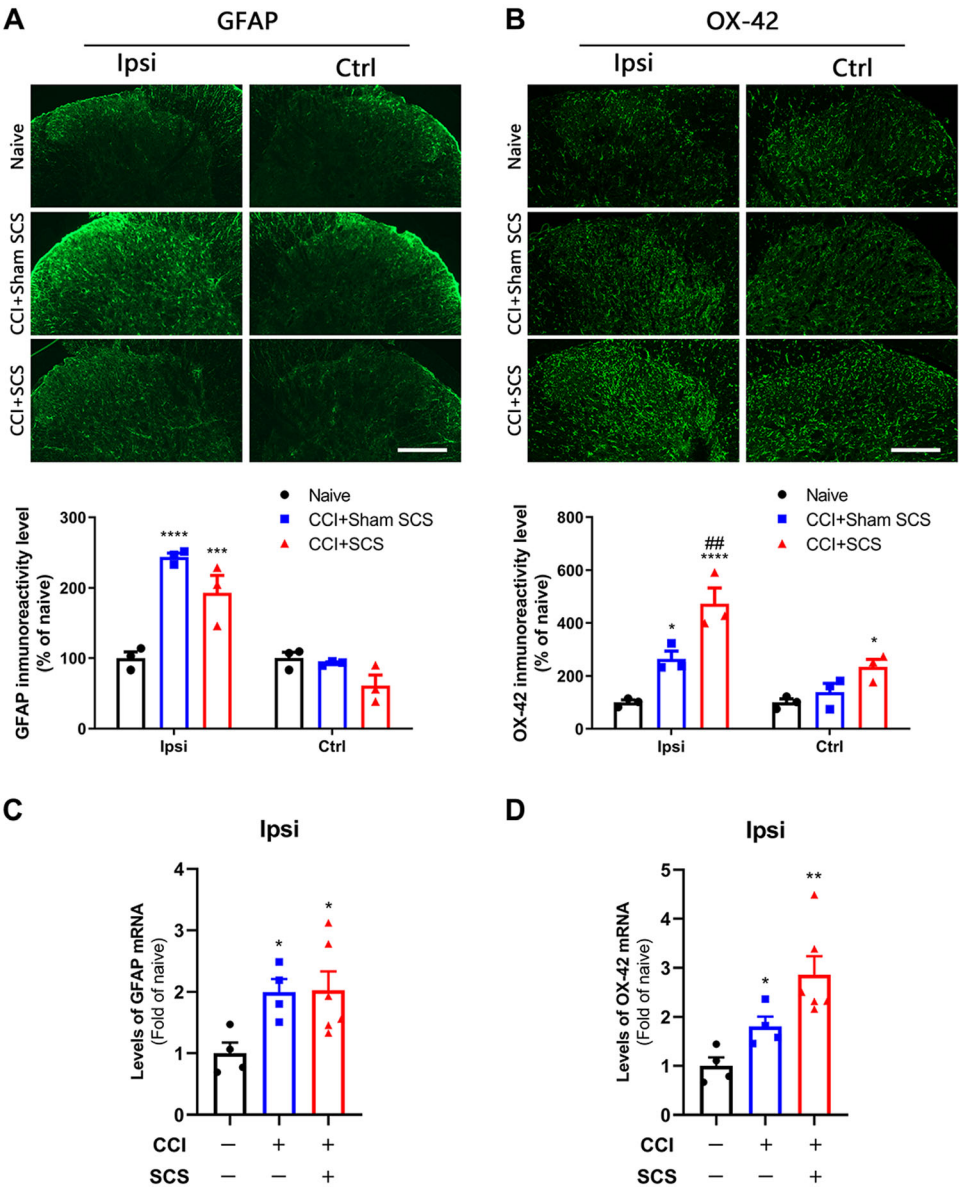

Fig. 2 Changes in the immunoreactivity and mRNA levels of GFAP and OX-42 in the spinal cord after CCI and SCS. **A** Upper: representative images of GFAP staining in the dorsal horn ipsilateral (Ipsi) and contralateral (Ctrl) to the nerve injury. Lower: quantification of GFAP immunoreactivity in each group. **B** Upper: representative images of OX-42 staining. Lower: quantification of OX-42 immunoreactivity. Scale bars, 100 μm. **C**, **D** Levels of GFAP mRNA (**C**) and OX-42 mRNA (**D**) in the ipsilateral cord of the different groups. n = 3–6 rats/group. Data are shown as the mean ± SEM. $^{*}P < 0.05$, $^{**}P < 0.01$, $^{***}P < 0.001$, $^{****}P < 0.0001$ *vs* naïve; $^{\#\#}P < 0.01$ *vs* CCI + Sham SCS; one-way ANOVA, with Bonferroni *post hoc* test.

SCS Changes Microglial Phenotypic Markers and Cytokine Levels in the Spinal Cord of CCI Rats

RT-PCR of the ipsilateral dorsal horn showed that the mRNA levels of CD16 and CD32 (M1-like markers) were significantly higher in sham-stimulated CCI rats than in naïve rats (Fig. 3A). In addition, SCS significantly increased the mRNA levels of both CD16 and iNOS mRNA in CCI rats. The mRNA levels of the pro-inflammatory cytokines IL-1β and TNF-α were similar in sham-stimulated CCI rats and naïve rats. However, the IL-1β mRNA level was significantly increased in CCI rats after SCS (Fig. 3B). The mRNA levels of the M2-like markers Arg1, CD163, and TGF-β were not significantly changed by CCI or SCS (Fig. 3C). However, the mRNA levels of the anti-inflammatory cytokines IL-4 and IL-10 were significantly lower in sham-stimulated CCI rats than in naïve rats. SCS did not significantly alter the IL-4 or IL-10 mRNA levels in CCI rats from those in sham-stimulated CCI rats (Fig. 3D; F = 4.39, iNOS; F = 13.34, CD16; F = 6.625, CD32; F = 4.36, IL-1β; F = 0.74, TNF-α; F = 0.39, Arg1; F = 1.01, CD163; F = 1.81, TGF-β; F = 12.99, IL-4; F = 10.92, IL-10).

Western blot analysis showed that the protein levels of iNOS, TNF-α, Arg1, and IL-10 did not differ significantly between sham-stimulated CCI and naïve rats. Repeated SCS in CCI rats upregulated iNOS expression (Fig. 4A), but did not change TNF-α, Arg1, or IL-10 expression (Fig. 4B–D), as compared to that in sham-stimulated rats (F = 4.49, iNOS; F = 1.27, TNF-α; F = 2.06, Arg1; F = 0.024, IL-10).

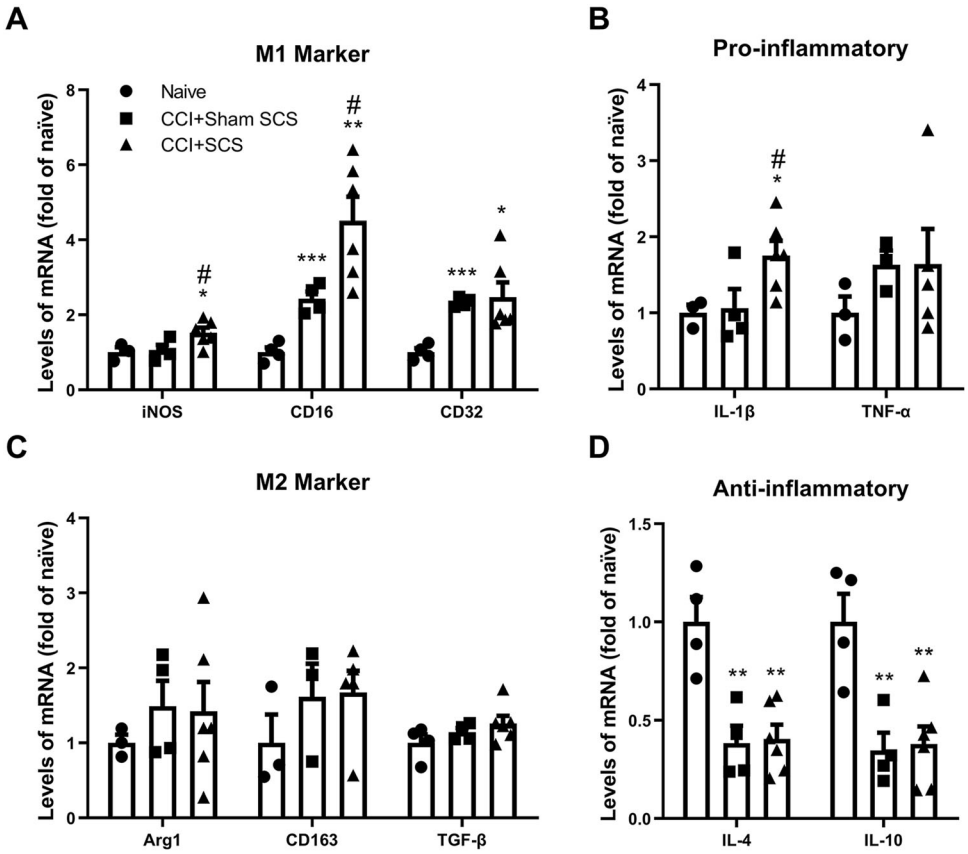

Fig. 3 Changes in the mRNA levels of M1-like and M2-like microglia markers and related cytokines in the ipsilateral spinal cord after CCI and SCS. **A** Levels of iNOS, CD16, and CD32 mRNA. **B** Levels of IL-1β and TNF-α mRNA. **C** Levels of Arg1, CD163, and TGF-β mRNA. **D** Levels of IL-4 and IL-10 mRNA. n = 3–6 rats/group. Data are shown as the mean ± SEM. $^{*}P < 0.05$, $^{**}P < 0.01$, $^{***}P < 0.001$ *vs* naïve; $^{\#}P < 0.05$ *vs* CCI + Sham SCS; one-way ANOVA, with Bonferroni *post hoc* test.

Effects of SCS on the Expression of Pro-nociceptive Molecules in the Spinal Cord of CCI Rats

Phosphorylated (p-) forms of NR1 (p-NR1), GluR1 (p-GluR1^{ser831}), and extracellular signal-regulated kinase (p-ERK1/2) are neurochemical markers for central sensitization [30–32]. Thus, in addition to the M1-like markers associated with microglial polarization, we examined the protein levels of these pro-nociceptive molecules in the spinal cord. Western blot analysis showed that the p-ERK1/2 levels were significantly higher in the ipsilateral cord of sham-stimulated CCI rats than in that of naïve rats (Fig. 5A). However, the protein levels of c-Fos, BDNF, PKC-γ, p-NR1, and p-GluR1^{ser831} did not differ significantly between the two groups (Fig. 5B–F). Compared to sham stimulation, SCS significantly decreased the BDNF levels in CCI rats (Fig. 5C; $F = 12.31$, p-ERK1/2; $F = 0.61$, c-Fos; $F = 4.55$, BDNF; $F = 0.37$, PKC-γ; $F = 0.39$, p-NR1; $F = 3.45$, p-GluR1).

Intrathecal Injection of Minocycline Prolongs Pain Inhibition by SCS

Lastly, we determined whether inhibiting microglial activation in the spinal cord affects pain inhibition by SCS in CCI rats. Intrathecal administration of minocycline, a microglial inhibitor, dose-dependently attenuated mechanical hypersensitivity in the ipsilateral hind paw of CCI rats (Fig. 6A; $F = 5.79$, group; $F = 228.7$, time; $F = 4.20$, group–time interaction). Based on previous studies [6, 33], we tested three minocycline doses (1 μg, 10 μg, 100 μg/15 μL). At the highest dose, the ipsilateral PWT was significantly increased from pre-drug baseline from 30 min–150 min post-drug; lower doses were not effective.

Based on these findings, we tested the combination of low-dose minocycline (1 μg, i.t.) and SCS. Rats underwent CCI surgery and SCS electrode implantation on the same day and were randomized to receive SCS+minocycline (n = 15), SCS+vehicle (n = 15), or sham stimulation (n = 7) on day 18 post-CCI. SCS (50 Hz, 0.2 ms, biphasic, constant current, 80% MoT, 120 min) was delivered at 30 min after pretreatment with drug or vehicle. PWT was measured 1 day before CCI, before SCS and intrathecal injection (pre-SCS), during SCS (intra-SCS, 30 min, 60 min, and 120 min), and after SCS (30 min, 60 min, and 120 min). SCS increased the ipsilateral PWTs from pre-SCS levels in CCI rats that received either vehicle or minocycline, with a peak effect at ∼60 min–120 min intra-SCS in both groups. The pain-inhibiting effect diminished quickly after SCS cessation in the vehicle-pretreated group. Notably, pretreatment with 1 μg minocycline prolonged the SCS-induced pain inhibition, as

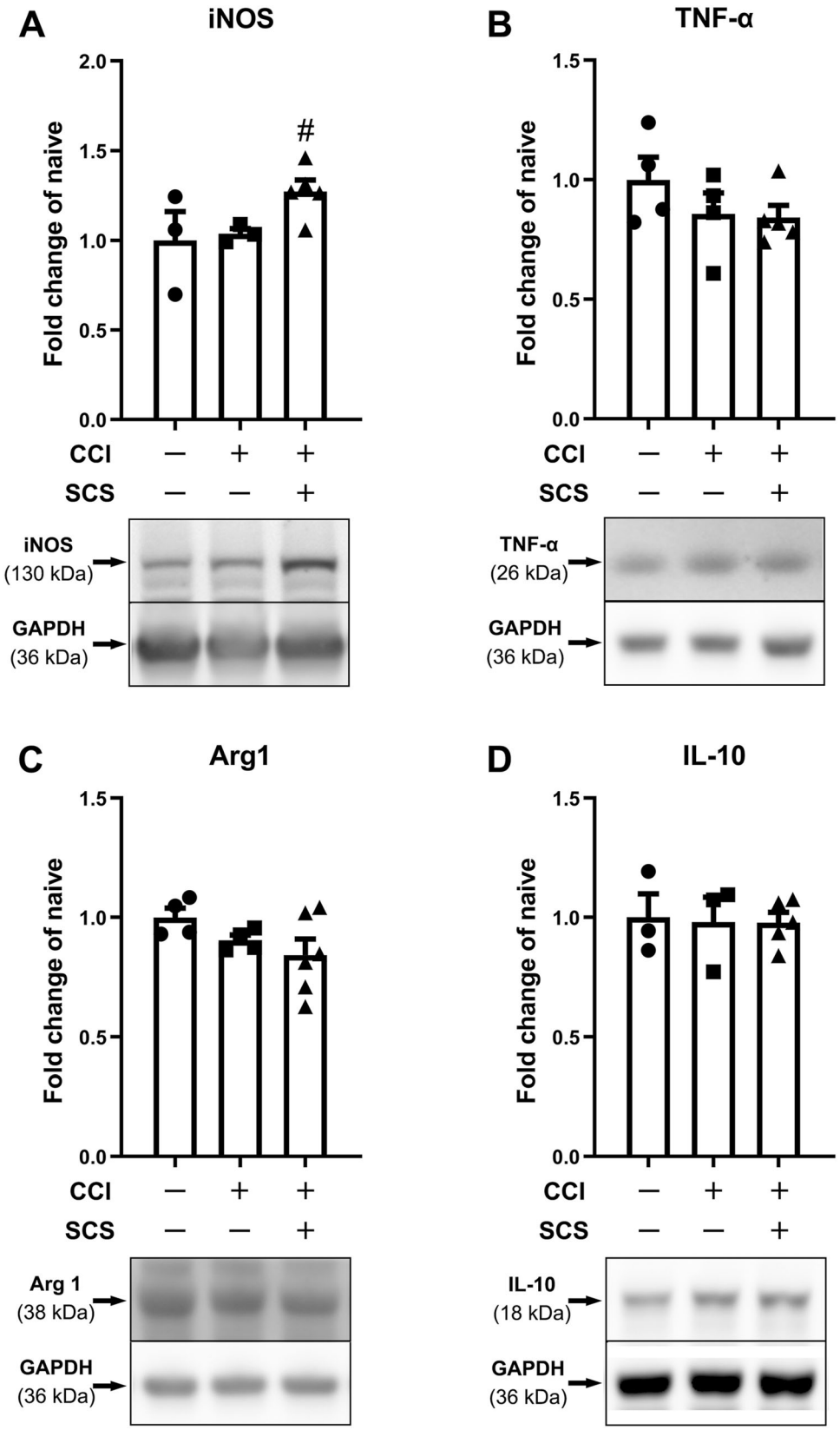

Fig. 4 Changes in the levels of M1-like and M2-like microglial markers and related cytokines in the ipsilateral spinal cord after CCI and SCS. Quantification (upper) and representative immunoblots (lower) of (**A**) iNOS, (**B**) TNF-α, (**C**) Arg1, and (**D**) IL-10 in different groups. $n = 3$–6 rats/group. Data are shown as the mean ± SEM. $^{\#}P < 0.05$ *vs* CCI + Sham SCS; one-way ANOVA, with Bonferroni *post hoc* test.

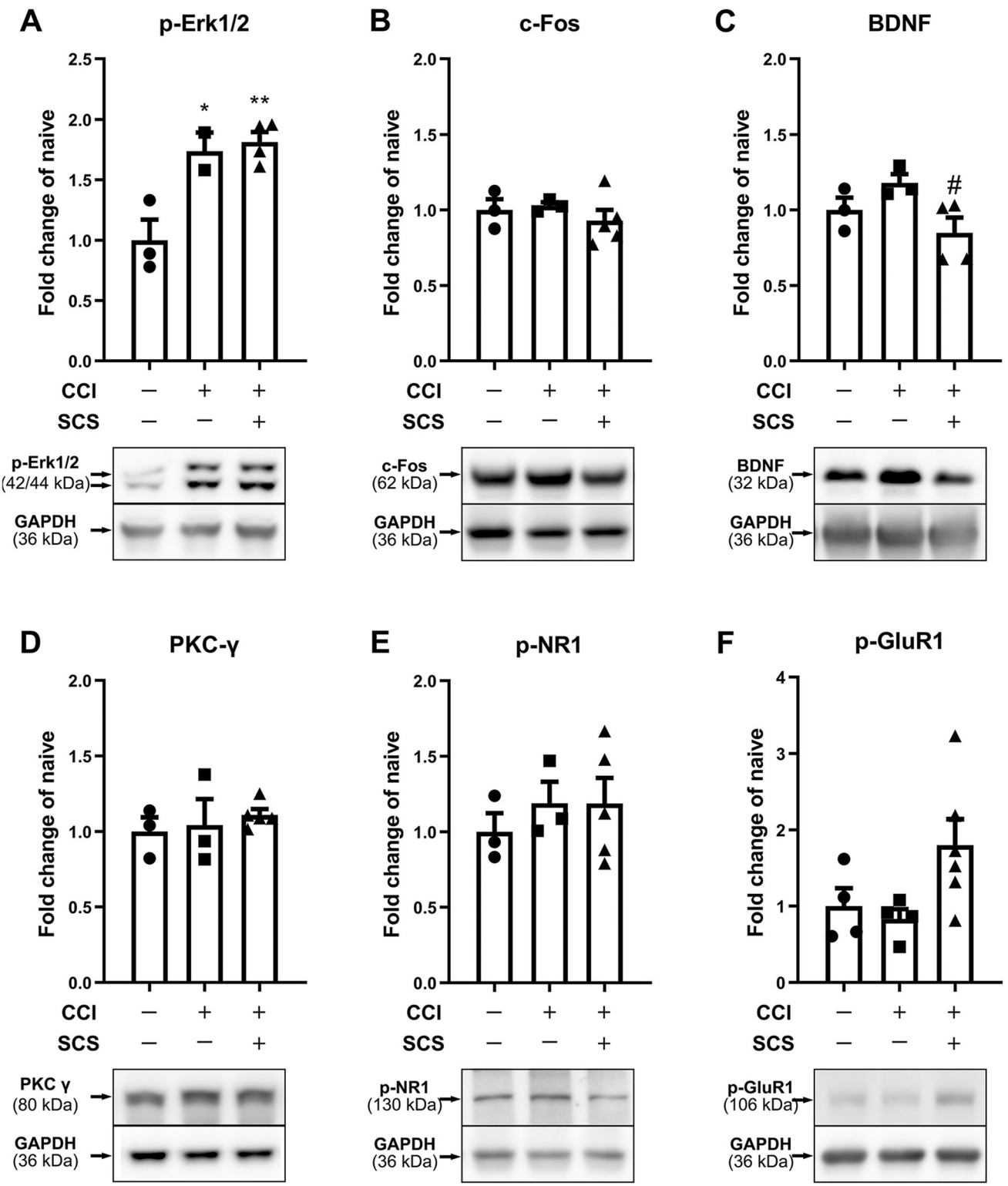

Fig. 5 Changes in the protein levels of pro-nociceptive factors in the ipsilateral spinal cord after CCI and SCS. Quantification (upper) and representative immunoblots (lower) of (**A**) p-ERK1/2, (**B**) c-fos, (**C**) BDNF, (**D**) PKC-γ, (**E**) p-NR1, and (**F**) p-GluR1^{ser831} in different groups. $n = 3$–6 rats/group. Data are shown as the mean ± SEM. $^{*}P < 0.05$, $^{**}P < 0.01$ *vs* naïve; $^{\#}P < 0.05$ *vs* CCI + Sham SCS; one-way ANOVA, with Bonferroni *post hoc* test.

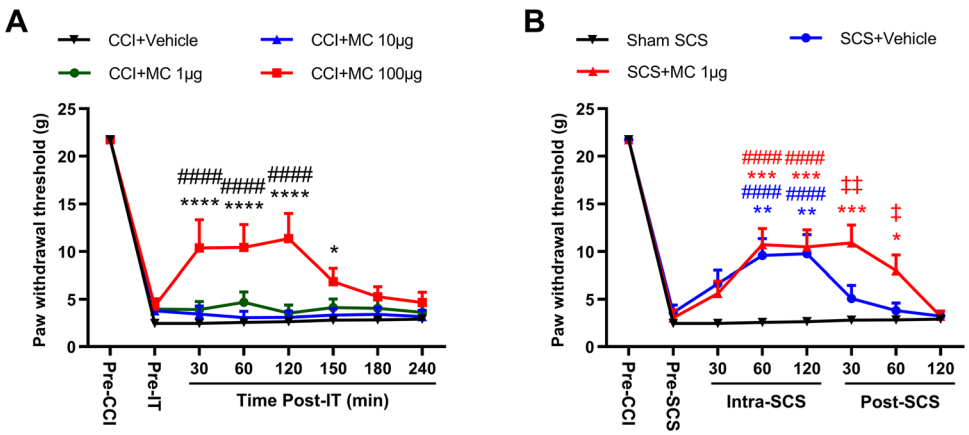

Fig. 6 Intrathecal administration of low-dose minocycline (MC) prolongs the pain inhibition induced by SCS in CCI rats. **A** Ipsilateral paw withdrawal thresholds (PWTs) of CCI rats after intrathecal injection of vehicle ($n = 7$) or minocycline (1 μg, 10 μg, or 100 μg, 15 μL, $n = 9$ or 10/dose). PWT was measured one day before CCI (Pre-CCI), before intrathecal injection (Pre-IT), and at 30 min, 60 min, 120 min, 150 min, 180 min, and 240 min post-injection (Post-IT) on day 18 post-CCI. Data are shown as the mean ± SEM. $^{*}P < 0.05$, $^{****}P < 0.0001$ *vs* CCI + Vehicle; $^{\#\#\#\#}P < 0.0001$ *vs* Pre-IT; two-way mixed model ANOVA, with Bonferroni *post hoc* test. **B** PWTs after sham SCS ($n = 7$) or SCS in CCI rats pretreated (30 min) with an intrathecal injection of low-dose minocycline (1 μg, 15 μL, $n = 16$) or vehicle ($n = 15$). PWT was measured one day before CCI (Pre-CCI), before SCS and intrathecal injection (Pre-SCS), during SCS (Intra-SCS; 30 min, 60 min, and 120 min) and after SCS (Post-SCS; 30 min, 60 min, and 120 min) on day 18 post-CCI. Data are shown as the mean ± SEM. $^{*}P < 0.05$, $^{**}P < 0.01$, $^{***}P < 0.001$ *vs* Sham SCS; $^{\#\#\#\#}P < 0.0001$ *vs* Pre-SCS; $^{\ddagger}P < 0.05$, $^{\ddagger\ddagger}P < 0.01$ *vs* SCS + Vehicle; two-way mixed model ANOVA, with Bonferroni *post hoc* test.

compared to that with vehicle pretreatment (Fig. 6B; $F = 3.73$, group; $F = 101.4$, time; $F = 4.11$, group–time interaction).

Discussion

Both microglia and astrocytes in the spinal cord are thought to play an important role in neuropathic pain conditions [34, 35]. We found that at 3 weeks after rats underwent sciatic CCI, the ipsilateral lumbar spinal cord exhibited higher levels of OX-42 and GFAP immunoreactivity and mRNA than those of naïve rats, suggesting that both microglia and astrocytes remain activated at this maintenance phase of neuropathic pain. Repeated SCS did not significantly alter GFAP immunoreactivity or mRNA levels in the ipsilateral lumbar spinal cord of CCI rats. However, it further increased the immunoreactivity of OX-42, a marker of reactive microglia, in the bilateral dorsal horns of CCI rats. SCS also produced a trend toward increased OX-42 mRNA in the ipsilateral spinal cord. Thus, conventional SCS did not suppress the heightened astrocyte and microglial activation, but may have exacerbated microglial activation in the lumbar cord of CCI rats during the maintenance phase of neuropathic pain. This finding is in line with previous findings that continuous conventional SCS (72 h) in uninjured rats increases the GFAP and ITGAM (OX-42) genes in the lumbar cord, as compared to sham stimulation, suggesting elevated glia-related mRNA in the spinal cord [36]. However, another study showed that 4 consecutive days of SCS attenuated glial activation in a spared nerve injury model of neuropathic pain, as indicated by decreased GFAP, MCP-1, and OX-42 immunoreactivity in the dorsal horn [19]. The reason for this discrepancy is unclear but may be due in part to differences in the animal models, post-injury time points, and SCS protocols between these studies.

How SCS increases OX-42 expression remains unclear. It is possible that conventional SCS may induce the release of ATP from neurons into the spinal cord, which would activate P2X7 and P2X4 receptors on microglial cells [37, 38]. Importantly, our RT-PCR study also showed that the SCS-induced increase in microglial activation was associated with differential changes in M1-like and M2-like phenotypic markers. Specifically, the mRNA levels of M1-like markers, such as iNOS and CD16, were significantly increased in CCI rats that received SCS, as compared to the levels in sham-stimulated rats. The increase in iNOS mRNA was also associated with increased protein expression. However, SCS did not alter the mRNA of some M2-like markers, such as Arg1, CD163, and TGF-β. In line with these findings, the mRNA levels of the pro-inflammatory cytokine IL-1β was also increased in CCI rats after SCS, whereas the mRNA levels of the anti-inflammatory cytokines IL-4 and IL-10, which decreased after CCI, were not changed by SCS. These

findings suggest that SCS may promote the pro-inflammatory M1-like phenotype of microglia in the spinal cord after nerve injury. This notion supports findings in a recent RNA-sequencing study, which showed that repetitive SCS further increases the mRNA levels of many immune-related genes, including genes encoding markers for astrocytes (*Gfap* and *Ccl2*) and activated microglia (*Cd68* and *Itgam*) in the lumbar spinal cord of CCI rats [21].

Pro-inflammatory cytokines such as IL-1β and TNF-α released from microglia can increase neural activity and activate neighboring glial cells. In addition, activated microglia may function to clear various neurotransmitters, including the pain-inhibitory gamma-aminobutyric acid (GABA) that is released during SCS [39, 40]. Hence, increased activation of M1-like microglia may compromise the pain-inhibiting actions of SCS. Nevertheless, the expression of c-Fos, PKC-γ, p-NR1, and p-GluR1^{ser831}, which are common markers of neuronal activation and sensitization, were not increased in CCI rats after SCS. In fact, SCS decreased the protein level of BDNF, which contributes to central sensitization by converting GABAergic inhibitory cells to excitation *via* TrkB-KCC2 [38] and by potentiating glutamatergic excitation *via* NMDA receptors. Thus, a decrease in BDNF expression may contribute to SCS-induced pain inhibition. Taken together, these findings suggest that conventional SCS induces a mixture of neurochemical changes in the spinal cord that involve immune and glial reactions.

Although microglia can be categorized into classically activated (M1-like) and alternatively activated (M2-like) states [41], *in vivo* these states may occur on a spectrum of functionality [41] that is context-dependent under different pathological conditions [42, 43]. Mounting evidence indicates that the net effect of microglial activation in the spinal cord contributes to neuropathic pain [44]. Minocycline is a tetracycline antibiotic that preferentially inhibits the proinflammatory actions of activated microglia, as neurons and astrocytes are more resistant to its metabolic effects. Minocycline has also been shown to inhibit chemotherapy-induced peripheral neuropathy and bone cancer pain by inhibiting the nuclear factor-κB signaling pathway in astrocytes [45]. Besides inhibition of glial activation or function, minocycline can also alter spinal endocannabinoids [46], reduce the impairment of glial glutamate uptake [47], inhibit phosphorylation of neuronal ERK1/2 [48], and promote microglial M1-like to M2-like gene expression [33]. Indeed, intrathecal injection of minocycline dose-dependently inhibited the mechanical hypersensitivity in CCI rats. This finding supports previous observations [6, 49] and suggests that the net outcome of microglial activation may be pain facilitation at 3 weeks post-CCI. SCS increased the mechanical PWT in CCI rats from the pre-SCS level, but this effect was short-lived. Importantly, pretreating rats with an intrathecal injection of a sub-effective minocycline dose prolonged the pain inhibition by SCS.

Clinically, pain relief by conventional, low-frequency (40 Hz–60 Hz) SCS often requires a high amplitude that elicits paresthesia (i.e., above the sensory threshold) in patients [11, 14]. Animal studies have also shown that decreasing the stimulation intensity to 20%–40% MoT markedly reduces the pain-inhibiting effect of conventional SCS [15–17]. The mode of action for conventional SCS involves feed-forward inhibition of dorsal horn neurons [10, 11, 16, 17]. Yet, whether it also depends on proper modulation or normalization of glial dysfunction and altered neuron-glia interactions is unclear. Collectively, the current findings suggest that SCS increases M1-like microglial activation in the spinal cord, which may counteract its pain inhibitory action. Recently, DTMP SCS was shown to induce greater pain inhibition than conventional SCS, perhaps owing to more effective modulation of gene expression and biological processes associated with glial function and neuron-glial interactions [18]. These findings suggest that the efficacy of SCS may be improved by developing new SCS paradigms that better modulate spinal glial function. As an anti-inflammatory drug, minocycline may also enhance SCS-induced pain inhibition through other neuronal mechanisms, such as by inhibiting sodium currents in dorsal root ganglion neurons [5]. However, the administration of low-dose minocycline alone did not inhibit pain, suggesting that this neuronal mechanism may not contribute to the enhancement of SCS-induced pain inhibition.

Our study has some limitations. First, we examined only the conventional SCS paradigm. Therefore, the effects of high-frequency, sub-sensory threshold SCS and burst SCS on spinal glial phenotypes and functions must still be studied. In addition, because of technical challenges, we used intermittent rather than continuous SCS (48–72 h), which is usually used in the clinic and has been tested in previous animal studies [18, 22, 36]. It is plausible that microglial modulation and its impact on pain may differ for different stimulation time schemes and paradigms. In addition, because tissues from CCI rats treated with minocycline and SCS were not harvested for RT-PCR and Western blotting, it remains to be determined whether the improvement in pain inhibition is attributable to enhanced inhibition of microglial activation.

SCS has more than 50 years of history as a useful non-pharmacological intervention for chronic pain. Although the clinical use of SCS continues to grow, studies of the biological and neurochemical mechanisms underlying SCS-induced analgesia have lagged behind. Most previous studies of SCS-induced analgesia have revolved around neuronal mechanisms in spinal and supraspinal structures,

and identified many neurochemical mechanisms, including serotonin, epinephrine, GABA, acetylcholine, adenosine, and endocannabinoids [10, 11, 50]. Comparatively, our knowledge about the roles of non-neuronal mechanisms in the therapeutic effects of SCS remains limited. Our current findings show that repeated SCS may increase M1-like microglial activation in the spinal cord of nerve-injured rats and suggest that inhibition of microglial activation or promotion of M2-like polarization with adjuvant pharmacotherapy may present an opportunity to prolong the pain inhibition of conventional SCS. Nevertheless, other M1- and M2-like polarization markers, and changes in the associated cytokines in the spinal cord after SCS warrant future investigation. This study represents a continuing effort toward understanding the non-neuronal modulatory actions of SCS [21, 22, 51], which may spur the clinical development of mechanism-based interventions to improve its therapeutic effects.

Acknowledgements We thank Claire F. Levine, MS, ELS (Scientific Editor, Department of Anesthesiology and Critical Care Medicine, Johns Hopkins University), for editing the manuscript and Medtronic, Inc. (Minneapolis, MN, USA) for generously providing the rodent electrodes for spinal cord stimulation. This work was supported by a grant from the Neurosurgery Pain Research Institute at the Johns Hopkins University and subsidized by the National Institutes of Health (Bethesda, Maryland, USA) (NS110598). The efforts of B.S. were supported by an award from the China Scholarship Council for Chinese PhD candidates to study abroad.

Conflict of interest Dr. Yun Guan received research grant support from Medtronic, Inc., Minneapolis, MN. However, none of the authors has a commercial interest in the material presented in this paper. There are no other relationships that might lead to a conflict of interest in the current study. The authors declare no competing interests.

References

1. Watkins LR, Hutchinson MR, Ledeboer A, Wieseler-Frank J, Milligan ED, Maier SF. Norman Cousins Lecture. Glia as the "bad guys": implications for improving clinical pain control and the clinical utility of opioids. Brain Behav Immun 2007, 21: 131–146.
2. Crain JM, Nikodemova M, Watters JJ. Microglia express distinct M1 and M2 phenotypic markers in the postnatal and adult central nervous system in male and female mice. J Neurosci Res 2013, 91: 1143–1151.
3. Nikodemova M, Watters JJ. Efficient isolation of live microglia with preserved phenotypes from adult mouse brain. J Neuroinflammation 2012, 9: 147.
4. Inoue K, Tsuda M. Microglia in neuropathic pain: cellular and molecular mechanisms and therapeutic potential. Nat Rev Neurosci 2018, 19: 138–152.
5. Mika J, Zychowska M, Popiolek-Barczyk K, Rojewska E, Przewlocka B. Importance of glial activation in neuropathic pain. Eur J Pharmacol 2013, 716: 106–119.
6. Ledeboer A, Sloane EM, Milligan ED, Frank MG, Mahony JH, Maier SF, *et al.* Minocycline attenuates mechanical allodynia and proinflammatory cytokine expression in rat models of pain facilitation. Pain 2005, 115: 71–83.
7. Chen G, Luo X, Qadri MY, Berta T, Ji RR. Sex-Dependent Glial Signaling in Pathological Pain: Distinct Roles of Spinal Microglia and Astrocytes. Neurosci Bull 2018, 34: 98–108.
8. Tsuda M. Modulation of Pain and Itch by Spinal Glia. Neurosci Bull 2018, 34: 178–185.
9. Kumar K, Taylor RS, Jacques L, Eldabe S, Meglio M, Molet J, *et al.* Spinal cord stimulation versus conventional medical management for neuropathic pain: a multicentre randomised controlled trial in patients with failed back surgery syndrome. Pain 2007, 132: 179–188.
10. Barchini J, Tchachaghian S, Shamaa F, Jabbur SJ, Meyerson BA, Song Z, *et al.* Spinal segmental and supraspinal mechanisms underlying the pain-relieving effects of spinal cord stimulation: an experimental study in a rat model of neuropathy. Neuroscience 2012, 215: 196–208.
11. Foreman RD, Linderoth B. Neural mechanisms of spinal cord stimulation. Int Rev Neurobiol 2012, 107: 87–119.
12. Sivanesan E, Maher DP, Raja SN, Linderoth B, Guan Y. Supraspinal Mechanisms of Spinal Cord Stimulation for Modulation of Pain: Five Decades of Research and Prospects for the Future. Anesthesiology 2019, 130: 651–665.
13. Huang Q, Duan W, Sivanesan E, Liu S, Yang F, Chen Z, *et al.* Spinal Cord Stimulation for Pain Treatment After Spinal Cord Injury. Neurosci Bull 2019, 35: 527–539.
14. Sdrulla AD, Guan Y, Raja SN. Spinal Cord Stimulation: Clinical Efficacy and Potential Mechanisms. Pain Pract 2018, 18: 1048–1067.
15. Yang F, Xu Q, Cheong YK, Shechter R, Sdrulla A, He SQ, *et al.* Comparison of intensity-dependent inhibition of spinal wide-dynamic range neurons by dorsal column and peripheral nerve stimulation in a rat model of neuropathic pain. Eur J Pain 2014, 18: 978–988.
16. Shechter R, Yang F, Xu Q, Cheong YK, He SQ, Sdrulla A, *et al.* Conventional and kilohertz-frequency spinal cord stimulation produces intensity- and frequency-dependent inhibition of mechanical hypersensitivity in a rat model of neuropathic pain. Anesthesiology 2013, 119: 422–432.
17. Guan Y. Spinal cord stimulation: neurophysiological and neurochemical mechanisms of action. Curr Pain Headache Rep 2012, 16: 217–225.
18. Vallejo R, Kelley CA, Gupta A. Modulation of neuroglial interactions using differential target multiplexed spinal cord stimulation in an animal model of neuropathic pain. Mol Pain 2020, 16: 1744806920918057.
19. Sato KL, Johanek LM, Sanada LS, Sluka KA. Spinal cord stimulation reduces mechanical hyperalgesia and glial cell activation in animals with neuropathic pain. Anesth Analg 2014, 118: 464–472.
20. Sivanesan E, Stephens KE, Huang Q, Chen Z, Ford NC, Duan W, *et al.* Spinal cord stimulation prevents paclitaxel-induced mechanical and cold hypersensitivity and modulates spinal gene expression in rats. Pain Rep 2019, 4: e785.
21. Stephens KE, Chen Z, Sivanesan E, Raja SN, Linderoth B, Taverna SD, *et al.* RNA-seq of spinal cord from nerve-injured rats after spinal cord stimulation. Mol Pain 2018, 14: 1744806918817429.
22. Vallejo R, Tilley DM, Cedeno DL, Kelley CA, DeMaegd M, Benyamin R. Genomics of the Effect of Spinal Cord Stimulation on an Animal Model of Neuropathic Pain. Neuromodulation 2016, 19: 576–586.
23. Bennett GJ, Xie YK. A peripheral mononeuropathy in rat that produces disorders of pain sensation like those seen in man. Pain 1988, 33: 87–107.

24. Chaplan SR, Bach FW, Pogrel JW, Chung JM, Yaksh TL. Quantitative assessment of tactile allodynia in the rat paw. J Neurosci Methods 1994, 53: 55–63.
25. Dixon WJ. Efficient analysis of experimental observations. Annu Rev Pharmacol Toxicol 1980, 20: 441–462.
26. Yang F, Xu Q, Shu B, Tiwari V, He SQ, Vera-Portocarrero LP, *et al.* Activation of cannabinoid CB1 receptor contributes to suppression of spinal nociceptive transmission and inhibition of mechanical hypersensitivity by Abeta-fiber stimulation. Pain 2016, 157: 2582–2593.
27. Mestre C, Pelissier T, Fialip J, Wilcox G, Eschalier A. A method to perform direct transcutaneous intrathecal injection in rats. J Pharmacol Toxicol Methods 1994, 32: 197–200.
28. Liu S, Huang Q, He S, Chen Z, Gao X, Ma D, *et al.* Dermorphin [D-Arg2, Lys4] (1–4) amide inhibits below-level heat hypersensitivity in mice after contusive thoracic spinal cord injury. Pain 2019, 160: 2710–2723.
29. He SQ, Xu Q, Tiwari V, Yang F. Oligomerization of MrgC11 and μ-opioid receptors in sensory neurons enhances morphine analgesia. Sci Signal 2018, 11(535):eaao3134. https://doi.org/10.1126/scisignal.aao3134.
30. Ji RR, Befort K, Brenner GJ, Woolf CJ. ERK MAP kinase activation in superficial spinal cord neurons induces prodynorphin and NK-1 upregulation and contributes to persistent inflammatory pain hypersensitivity. J Neurosci 2002, 22: 478–485.
31. Zhuang ZY, Gerner P, Woolf CJ, Ji RR. ERK is sequentially activated in neurons, microglia, and astrocytes by spinal nerve ligation and contributes to mechanical allodynia in this neuropathic pain model. Pain 2005, 114: 149–159.
32. Woolf CJ, Mannion RJ. Neuropathic pain: aetiology, symptoms, mechanisms, and management. Lancet 1999, 353: 1959–1964.
33. Burke NN, Kerr DM, Moriarty O, Finn DP, Roche M. Minocycline modulates neuropathic pain behaviour and cortical M1-M2 microglial gene expression in a rat model of depression. Brain Behav Immun 2014, 42: 147–156.
34. Ji RR, Berta T, Nedergaard M. Glia and pain: Is chronic pain a gliopathy? Pain 2013, 154: S10–S28.
35. Raghavendra V, Tanga F, DeLeo JA. Inhibition of microglial activation attenuates the development but not existing hypersensitivity in a rat model of neuropathy. J Pharmacol Exp Ther 2003, 306: 624–630.
36. Tilley DM, Cedeño DL, Kelley CA, Benyamin R, Vallejo R. Spinal Cord Stimulation Modulates Gene Expression in the Spinal Cord of an Animal Model of Peripheral Nerve Injury. Reg Anesth Pain Med 2016, 41: 750–756.
37. Trang T, Beggs S, Wan X, Salter MW. P2X4-receptor-mediated synthesis and release of brain-derived neurotrophic factor in microglia is dependent on calcium and p38-mitogen-activated protein kinase activation. J Neurosci 2009, 29: 3518–3528.
38. Coull JA, Beggs S, Boudreau D, Boivin D, Tsuda M, Inoue K, *et al.* BDNF from microglia causes the shift in neuronal anion gradient underlying neuropathic pain. Nature 2005, 438: 1017–1021.
39. Stiller CO, Cui JG, O'Connor WT, Brodin E, Meyerson BA, Linderoth B. Release of gamma-aminobutyric acid in the dorsal horn and suppression of tactile allodynia by spinal cord stimulation in mononeuropathic rats. Neurosurgery 1996, 39: 367–374; discussion 374–365.
40. Cui JG, O'Connor WT, Ungerstedt U, Linderoth B, Meyerson BA. Spinal cord stimulation attenuates augmented dorsal horn release of excitatory amino acids in mononeuropathy via a GABAergic mechanism. Pain 1997, 73: 87–95.
41. Colonna M, Butovsky O. Microglia Function in the Central Nervous System During Health and Neurodegeneration. Annu Rev Immunol 2017, 35: 441–468.
42. Wes PD, Holtman IR, Boddeke EW, Moller T, Eggen BJ. Next generation transcriptomics and genomics elucidate biological complexity of microglia in health and disease. Glia 2016, 64: 197–213.
43. Zhang Y, Chen K, Sloan SA, Bennett ML, Scholze AR, O'Keeffe S, *et al.* An RNA-sequencing transcriptome and splicing database of glia, neurons, and vascular cells of the cerebral cortex. 2014, 34: 11929–11947.
44. Cao H, Zhang YQ. Spinal glial activation contributes to pathological pain states. Neurosci Biobehav Rev 2008, 32: 972–983.
45. Song ZP, Xiong BR, Guan XH, Cao F, Manyande A, Zhou YQ, *et al.* Minocycline attenuates bone cancer pain in rats by inhibiting NF-kappaB in spinal astrocytes. Acta Pharmacol Sin 2016, 37: 753–762.
46. Guasti L, Richardson D, Jhaveri M, Eldeeb K, Barrett D, Elphick MR, *et al.* Minocycline treatment inhibits microglial activation and alters spinal levels of endocannabinoids in a rat model of neuropathic pain. Mol Pain 2009, 5: 35.
47. Nie H, Zhang H, Weng HR. Minocycline prevents impaired glial glutamate uptake in the spinal sensory synapses of neuropathic rats. Neuroscience 2010, 170: 901–912.
48. Cho IH, Lee MJ, Jang M, Gwak NG, Lee KY, Jung HS. Minocycline markedly reduces acute visceral nociception via inhibiting neuronal ERK phosphorylation. Mol Pain 2012, 8: 13.
49. Pu S, Xu Y, Du D, Yang M, Zhang X, Wu J, *et al.* Minocycline attenuates mechanical allodynia and expression of spinal NMDA receptor 1 subunit in rat neuropathic pain model. J Physiol Biochem 2013, 69: 349–357.
50. Meyerson BA, Linderoth B. Mode of action of spinal cord stimulation in neuropathic pain. J Pain Symptom Manage 2006, 31: S6–12.
51. Tilley DM, Lietz CB, Cedeno DL, Kelley CA, Li L, Vallejo R. Proteomic Modulation in the Dorsal Spinal Cord Following Spinal Cord Stimulation Therapy in an In Vivo Neuropathic Pain Model. Neuromodulation 2020. https://doi.org/10.1111/ner.13103.